

**Supporting information for:**

**Crystallographic Structure Analysis of a Ti-Ta**

**Thin Film Materials Library Fabricated by**

**Combinatorial Magnetron Sputtering**

Peter M. Kadletz,<sup>\*,†</sup> Yahya Motemani,<sup>‡</sup> Joy Iannotta,<sup>†</sup> Steffen Salomon,<sup>‡</sup>  
Chinmay Khare,<sup>‡</sup> Lukas Grossmann,<sup>†</sup> Hans Jürgen Maier,<sup>¶</sup> Alfred Ludwig,<sup>‡</sup> and  
Wolfgang W. Schmahl<sup>†</sup>

*<sup>†</sup>Applied Crystallography and Materials Science, Department of Earth and Environmental  
Sciences, Faculty of Geosciences, Ludwig-Maximilians-Universität, 80333 München,  
Germany*

*<sup>‡</sup>Werkstoffe der Mikrotechnik, Institut für Werkstoffe, Ruhr-Universität Bochum, 44801  
Bochum, Germany*

*<sup>¶</sup>Institut für Werkstoffkunde (Materials Science), Leibniz Universität Hannover, 30823  
Garbsen, Germany*

E-mail: kadletz@lrz.uni-muenchen.de

# Contents

Mapping of the Chemical Composition and Thickness . . . . .	S3
Table of Refined Structure Parameters of $\alpha''$ , $\beta$ , Ta <sub>(tetr)</sub> and $\omega$ . . . . .	S3
Table of Phase Fractions of $\alpha''$ , $\beta$ , Ta <sub>(tetr)</sub> and $\omega$ . . . . .	S5
Table of Structure Models Employed in the Rietveld Refinement . . . . .	S6
Table of the Atomic Distribution in the $\omega$ Phase . . . . .	S6
Illustration of Residual Stress in the Materials Library . . . . .	S7

## Mapping of the Chemical Composition and Thickness

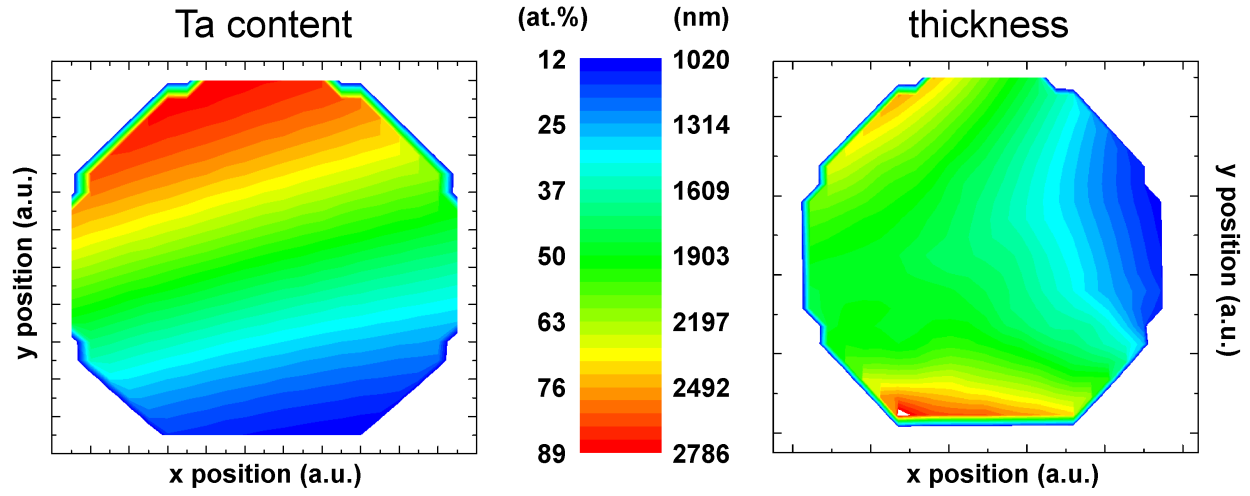


Figure S1: 2-dimensional mappings of the spatial chemical composition (left, in at.%) and thickness (right, in nm) of the sputtered Ti-Ta materials library. Orientation of the materials library is the same as in Figure 1 of the main document.

The thickness and the chemical composition were mapped over the entire area of the materials library (Figure S1). The thickness of the thin film ranges from  $\approx 1.0$  to  $\approx 2.8 \mu\text{m}$  and the chemical composition of the thin film ranges from  $\text{Ti}_{88}\text{Ta}_{12}$  to  $\text{Ti}_{11}\text{Ta}_{89}$ .

### Table of Refined Structure Parameters of $\alpha''$ , $\beta$ , $\text{Ta}_{(\text{tetr})}$ and $\omega$

Table S1 lists all structure parameters refined in the Rietveld fit of all four phases contained in the Ti-Ta materials library,  $\alpha''$ ,  $\beta$ ,  $\text{Ta}_{(\text{tetr})}$  and  $\omega$ . The list is ordered by the nominal averaged Ta-content of the measuring points P01 to P20 across the materials library. Structure parameters which are not listed in Table S1 were held fixed. Isotropic Debye-Waller factors were fixed to 0.8, phase fractions are shown in Table S2, microstructural parameters are shown in Figure 7 of the main document.  $R_{\text{wp}}$  values are the final weighted residual of the Rietveld fit and are listed in Table S1. Structure models taken for the Rietveld refinement are listed in Table S3.

Table S1: Refined structure parameters of all phases contained in the Ti-Ta materials library,  $\alpha''$ ,  $\beta$ ,  $\text{Ta}_{(\text{tetr})}$  and  $\omega$ , ordered by Ta-content of measuring points P1 to P20. Values were obtained by Rietveld refinement performed with the Rietveld software MAUD<sup>S1,S2</sup>.  $R_{\text{wp}}$  values are the final weighted residual of the Rietveld fit. Volume fractions are listed in Table S2.

#	$x_{\text{Ta}}$ (at.%)	$R_{\text{wp}}$ (%)	$\alpha''$				$\beta$	$\text{Ta}_{(\text{tetr})}$		$\omega$	
			$a$ (Å)	$b$ (Å)	$c$ (Å)	$y$	$a$ (Å)	$a$ (Å)	$c$ (Å)	$a$ (Å)	$c$ (Å)
P1	13.1	4.25	3.0163(1)	5.0174(2)	4.7068(2)	0.6886(1)	-	-	-	4.6285(8)	2.8313(3)
P2	15.9	4.14	3.0451(1)	4.9758(3)	4.6958(3)	0.6984(1)	-	-	-	-	-
P3	19.0	3.91	3.0769(2)	4.9317(3)	4.6745(3)	0.7022(1)	-	-	-	-	-
P4	21.9	4.71	3.1137(3)	4.8952(4)	4.6537(4)	0.7043(1)	-	-	-	-	-
P5	25.8	5.07	3.1563(3)	4.8281(4)	4.6294(5)	0.7167(1)	-	-	-	-	-
P6	29.6	4.38	3.2185(2)	4.7590(3)	4.6211(4)	0.7276(1)	-	-	-	-	-
P7	33.8	3.59	3.248(7)	4.708(2)	4.637(7)	0.735(3)	3.2746(1)	-	-	-	-
P8	38.1	5.29	3.258(6)	4.737(6)	4.640(8)	0.717(3)	3.2853(1)	-	-	-	-
P9	43.1	6.16	-	-	-	-	3.28191(9)	-	-	-	-
P10	48.0	7.03	-	-	-	-	3.2882(1)	-	-	-	-
P11	52.4	5.26	-	-	-	-	3.28807(6)	-	-	-	-
P12	57.6	2.05	-	-	-	-	3.28670(4)	10.1036(6)	5.2480(1)	-	-
P13	62.2	1.77	-	-	-	-	3.28713(4)	10.120(1)	5.2504(2)	-	-
P14	66.4	2.78	-	-	-	-	3.29166(6)	10.233(2)	5.2503(3)	-	-
P15	70.5	3.69	-	-	-	-	3.2913(1)	10.1438(6)	5.2442(3)	-	-
P16	74.4	2.66	-	-	-	-	3.29228(9)	10.1741(3)	5.2518(2)	-	-
P17	77.9	3.26	-	-	-	-	3.2914(1)	10.1930(4)	5.2532(3)	-	-
P18	80.7	4.01	-	-	-	-	3.29166(7)	10.1889(4)	5.26139(1)	-	-
P19	83.1	3.02	-	-	-	-	3.2956(1)	10.1540(3)	5.2770(3)	-	-
P20	85.6	2.92	-	-	-	-	3.3004(1)	10.1450(2)	5.2903(3)	-	-

## Table of Phase Fractions of $\alpha''$ , $\beta$ , $\text{Ta}_{(\text{tetr})}$ and $\omega$

Table S2 lists the volume fractions of  $\alpha''$ ,  $\beta$ ,  $\text{Ta}_{(\text{tetr})}$  and  $\omega$  contained in the materials library ordered by the nominal averaged chemical composition of measuring points P1 to P20.

Table S2: Volume fractions of measurements P1 – P20 and errors as resulting from the Rietveld refinement. Refined structural parameters are listed in Table S1.

#	$x_{\text{Ta}}$ (at.%)	volume fractions (%)				error (%)
		$\alpha''$	$\beta$	$\text{Ta}_{(\text{tetr})}$	$\omega$	
P1	13.1	98	-	-	2	$\pm 4$
P2–P6	15.9–29.6	100	-	-	-	-
P7	33.8	24	76	-	-	$\pm 2$
P8	38.1	3	97	-	-	$\pm 5$
P9–P11	43.1–52.4	-	100	-	-	-
P12	57.6	-	85	15	-	$\pm 1$
P13	62.2	-	94	6	-	$\pm 3$
P14	66.4	-	92	8	-	$\pm 2$
P15	70.5	-	68.5	31.5	-	$\pm 0.2$
P16	74.4	-	50.3	49.7	-	$\pm 0.2$
P17	77.9	-	33.8	66.2	-	$\pm 0.2$
P18	80.7	-	28.8	71.2	-	$\pm 0.3$
P19	83.1	-	17.9	82.1	-	$\pm 0.3$
P20	85.6	-	13.6	86.4	-	$\pm 0.1$

## Table of Structure Models Employed in the Rietveld Refinement

In Table S3 all structure models that were used in the Rietveld refinement are given.<sup>S3–S8</sup>

Table S3: Structure models employed in the Rietveld refinement.

phase	space group	no.	lattice constants (Å)	atoms on Wyckoff positions	Z (at.)	reference (material)
$\beta$	Im3m	229	$a = 3.2959(3)$	2a (0, 0, 0)	2	Neuburger <sup>S3</sup> (Ta)
$\alpha''$	Cmcm	63	$a = 3.166$ $b = 4.854$ $c = 4.652$	4c (0, y, $\frac{1}{4}$ ) $y \approx 0.2^{S4}$ or $0.6^{S5,S6}$	4	Brown et al. <sup>S4</sup> (Ti <sub>80</sub> Nb <sub>20</sub> )
$\omega$	P $\frac{6}{m}$ mm	191	$a = 4.60$ $c = 2.82$	1a (0, 0, 0) 2d ( $\frac{1}{3}, \frac{2}{3}, \frac{1}{2}$ )	3	Silcock et al. <sup>S7</sup> (Ti <sub>84</sub> V <sub>16</sub> )
Ta <sub>(tetr)</sub>	P4 <sub>2</sub> m	113	$a = 10.211(3)$ $c = 5.306(1)$	2c (0, $\frac{1}{2}$ , z) 4e, 4e, 4e (x, x+ $\frac{1}{2}$ , z) 8f, 8f (x, y, z)	30	Arakcheeva et al. <sup>S8</sup> (‘ $\beta$ -Ta’)

## Table of the Atomic Distribution in the $\omega$ Phase

In Table S4 the occupation probabilities  $P(\text{Ti})$  and  $P(\text{Ta})$  of Ti and Ta on Wyckoff positions  $1a$  and  $2d$  are given. Those values were obtained by Rietveld refinement of the  $\omega$  phase found in the P1 measurement (nominal composition: Ti<sub>87</sub>Ta<sub>13</sub>) of the materials library. The atomic distribution was determined by iteration of the Ti/Ta fraction until the lowest  $R_{\text{wp}}$ -value was reached in the Rietveld fit.

Table S4: Atomic distribution of the  $\omega$  phase found in measurement P1:  $P(\text{Ti})$  and  $P(\text{Ta})$  are the occupation probabilities of Ti and Ta on Wyckoff positions  $1a$  and  $2d$ .

position	Wyckoff	$P(\text{Ti})$	$P(\text{Ta})$
(0, 0, 0)	$1a$	75(5)	25(5)
( $\frac{1}{3}, \frac{2}{3}, \frac{1}{2}$ )	$2d$	95(5)	5(5)
whole unit cell		88(10)	12(10)

## Illustration of Residual Stress in the Materials Library

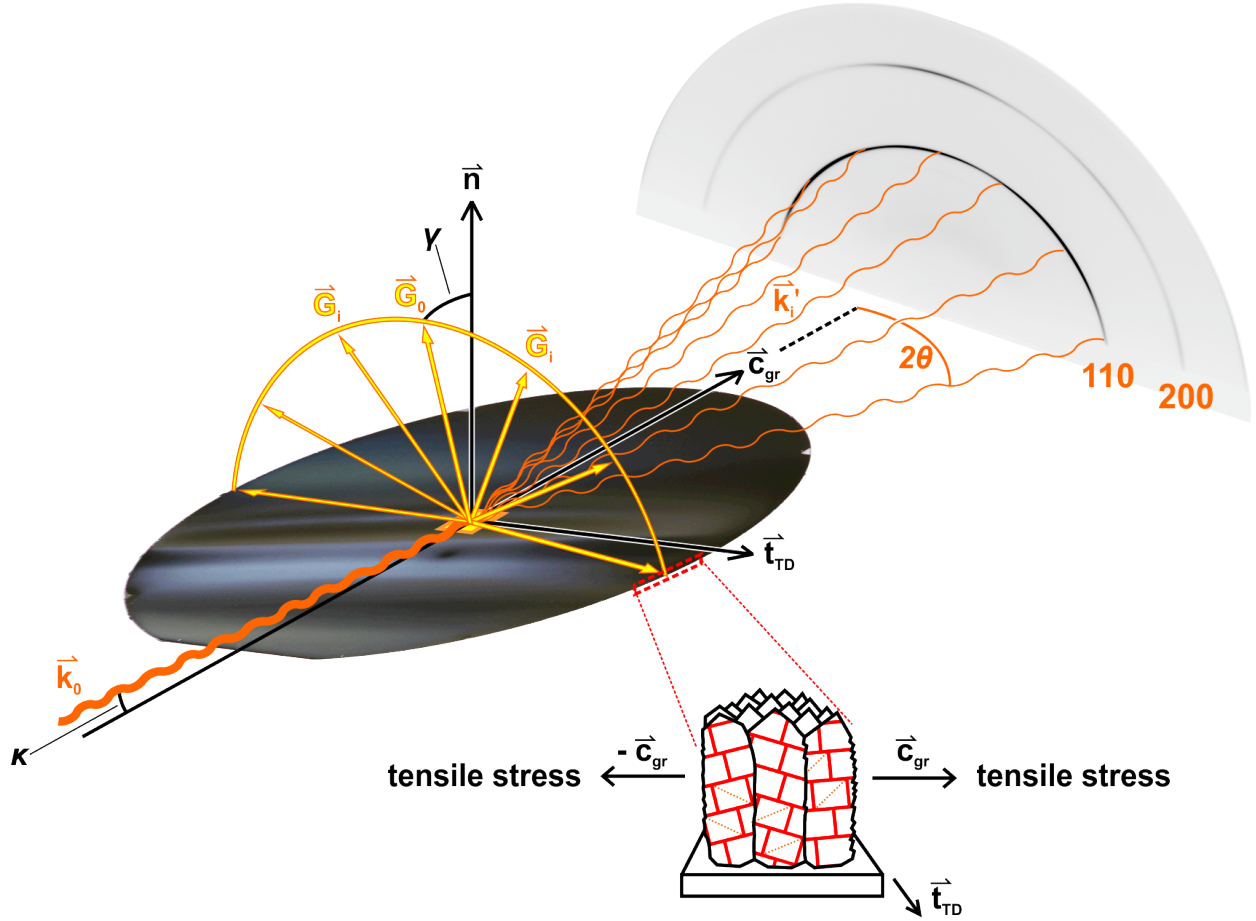


Figure S2: Distribution of scattering vectors  $\vec{G}_i$  in the GIXRD setup of the materials library and according stress state.  $\vec{k}_0$  is the incident beam,  $\vec{k}_i'$  are the beams diffracted by the polycrystalline surface of the materials library,  $\vec{G}_i$  (yellow arrows) indicate the resulting distribution of scattering vectors. The diffractogram (right) is the detector image from the P11 measurement, where only  $\beta$  is present, with reflections  $110_\beta$  and  $200_\beta$ . The Cartesian sample coordinate system is set by three basis vectors: the chemical gradient  $\vec{c}_{gr}$ , the transverse direction  $\vec{t}_{TD}$  and the normal direction  $\vec{n}$ .  $\kappa$  is the incidence angle,  $2\theta$  is the diffraction angle and  $\gamma$  is the inclination of  $\vec{G}_0$  from the normal direction  $\vec{n}$ . A schematic of the crystalline columns (bottom) illustrates ‘stretched’ d-spacing due to tensile stress acting along the chemical gradient  $\vec{c}_{gr}$ .

The residual stress state of the materials library can be inferred by analysis of the distribution of the sum of scattering vectors  $\vec{G}_i$  in the GIXRD setup, illustrated in Figure S2. Within the irradiated sample volume of the polycrystalline materials library  $\vec{G}_i$  represents the d-spacing

of all lattice planes that are in reflection condition. A scattering vector  $\vec{G}$  is perpendicular to a set of lattice planes in reflection condition and corresponds to the pole (= plane normal) of a lattice plane in a texture measurement. The coordinate system of the materials library is established by three basis vectors of a Cartesian coordinate system: the chemical gradient  $\vec{c}_{gr}$ , the transverse direction  $\vec{t}_{TD}$  and the normal direction  $\vec{n}$  (Figure S2). The direction of the chemical gradient  $\vec{c}_{gr}$  corresponds to the white arrow in Figure 1 (Ti- to Ta-rich) of the main document. For the static GIXRD setup the direction of  $\vec{G}_i$  can be approximated in a simple geometrical context by the inclination,  $\gamma$ , of  $\vec{G}_0$  from the perpendicular  $\vec{n}$  of the substrate:

$$\gamma = \frac{\kappa - 2\theta}{2} \quad (1)$$

where  $\kappa$  is the incidence angle of the primary beam and  $2\theta$  is the diffraction angle. For  $\gamma = 0$ ,  $\vec{G}$  points in the direction of  $\vec{n}$ , exactly perpendicular to the substrate; rotating  $\vec{G}$  around  $\vec{c}_{gr}$  would then create a plane with the normal vector  $\vec{c}_{gr}$ . The so created plane contains a radial distribution of  $\vec{G}_i$  representing the d-spacing within the distribution. In this study,  $\kappa = \text{const} = 3^\circ$  and  $2\theta$  takes values from  $13^\circ$  to  $25^\circ$ , therefore,  $\gamma$  takes values of  $-5^\circ$  to  $-11^\circ$ , which corresponds to a relatively small deviation from the substrate-perpendicular  $\vec{n}$ . Consequently, each detector image approximates a radial distribution of  $\vec{G}$  almost perpendicular to the chemical gradient of the materials library within the illuminated sample volume at points P1 to P20. Therefore, each 1D diffractogram, which was merged from caked and integrated slices of a detector image, represents an averaged d-spacing, distributed in  $\vec{G}_i$ , approximately perpendicular to the chemical gradient, which also involves the thickness direction (direction along the columns) of the materials library. The d-spacing of lattice planes within this radial distribution is overall reduced by compressive stress. This stress state could be caused by tensile stress acting along  $\vec{c}_{gr}$ , in-plane in the irradiated volume of the materials library.



## References

- (S1) Lutterotti, L.; Chateigner, D.; Ferrari, S.; Ricote, J. Texture, Residual Stress and Structural Analysis of Thin Films using a Combined X-Ray Analysis. *Thin Solid Films* **2004**, *450*, 34–41.
- (S2) Lutterotti, L. Total pattern fitting for the combined size–strain–stress–texture determination in thin film diffraction. *Nucl. Instrum. Methods Phys. Res., Sect. B* **2010**, *268*, 334 – 340.
- (S3) Neuburger, M. C. Präzisionsmessung der Gitterkonstante von sehr reinem Tantal. *Z. Kristallogr. - Cryst. Mater.* **1936**, *93*, 312 – 313.
- (S4) Brown, A. R. G.; Clark, D.; Eastabrook, J.; Jepson, K. S. The Titanium-Niobium System. *Nature* **1964**, *201*, 914–915.
- (S5) Moffat, D. L.; Larbalestier, D. C. The competition between martensite and omega in quenched Ti-Nb alloys. *Metall. Trans. A* **1988**, *19*, 1677–1686.
- (S6) Chakraborty, T.; Rogal, J.; Drautz, R. Martensitic transformation between competing phases in Ti–Ta alloys: a solid-state nudged elastic band study. *J. Phys.: Condens. Matter* **2015**, *27*, 115401.
- (S7) Silcock, J. M.; Davies, M. H.; Hardy, H. K. Structure of the  $\omega$ -Precipitate in Titanium-16 per cent Vanadium Alloy. *Nature* **1955**, *175*, 731.
- (S8) Arakcheeva, A.; Chapuis, G.; Grinevitch, V. The self-hosting structure of beta-Ta. *Acta Crystallogr., Sect. B: Struct. Sci., Cryst. Eng. Mater.* **2002**, *58*, 1–7.